The Large Programme "Cosmic Evolution of the IGM"

Metal enrichment, clustering properties and main heating process of the intergalactic medium can be probed by analyzing the numerous Lyman "forest" lines in the spectra of distant quasars and their associated, absorption metal lines. Constraints can then be placed on the scenarii of structure formation, the origin of metals and how they have been expelled in the intergalactic medium, and the spectral shape of the metagalactic UV flux.

J. Bergeron[1], P. Petitjean[1,2],
B. Aracil[3], C. Pichon[1],
E. Scannapieco[4], R. Srianand[5],
P. Boissé[1], R. F. Carswell[6],
H. Chand[5], S. Cristiani[7],
A. Ferrara[8], M. Haehnelt[6],
A. Hughes[1], T.-S. Kim[6],
C. Ledoux[9], P. Richter[10],
M. Viel[6]

[1]Institut d'Astrophysique de Paris, France
[2]LERMA, Observatoire de Paris, France
[3]Department of Astronomy, University of Massachusetts, USA
[4]Kavli Institute for Theoretical Physics, UC Santa Barbara, USA
[5]IUCAA, Pune, India
[6]Institute of Astronomy, Cambridge, UK
[7]INAF-Osservatorio Astronomico di Trieste, Italy
[8]SISSA/International School for Advanced Studies, Trieste, Italy
[9]European Southern Observatory
[10]Institut für Astrophysik und Extraterrestrische Forschung, Universität Bonn, Germany

The history of the Universe in its formative stages is recorded in the ubiquitous intergalactic medium (IGM), which contains almost all of the residual baryonic material from the Big Bang. During the epoch of structure formation, the IGM became highly inhomogeneous and acquired peculiar motions under the influence of gravity. It was the source of gas that accreted, and then cooled to form stars, and was also the sink for the metal-enriched gas and radiation produced by the population of primordial objects. Absorption lines in quasar spectra thus trace not only the chemical composition of the IGM, but also the density fluctuations in the early Universe and the background UV flux.

The IGM is revealed through numerous H I absorption lines in the spectra of remote quasars, the so-called Lyman-α forest. Numerical simulations and analytical modelling of a warm (~10^4 K) photoionised IGM within a cosmological context successfully reproduce many observational properties of the Lyman-α forest: the column density distribution, the Doppler parameter distribution, the flux decrement distribution and the redshift evolution of absorption lines above a certain column density threshold. Numerical hydro-simulations of CDM-based hierarchical structure formation have led to a new view of the IGM. In these models, structures arise from the action of gravity on density perturbations and the Lyman-α forest closely traces the density enhanced structures with geometrical shapes changing from sheets and filaments to more spherical halos as the column density increases.

The simulations have further demonstrated that the fluctuations of the neutral gas density responsible for the Lyman-α absorption trace the fluctuations in the underlying dark matter density field very well on scales larger than the Jeans length of the gas. In this paradigm, at $z \sim 2.5$ most of the baryons are located in somewhat overdense filaments and sheets, producing absorption in the column density range $10^{13.5} < N(\text{H I}) < 10^{15}$ cm^{-2}. However, most of the volume is occupied by underdense regions with typical column densities $N(\text{H I}) < 10^{13}$ cm^{-2}.

Concurrent with the progress in theoretical simulations, observations reveal that metal absorption features are associated with a considerable fraction of the high column density Lyman-α absorbers. The process responsible for the enrichment of the IGM is still only partially understood.

Considerable effort has been devoted to detect metal species associated with low column density Lyman-α systems, since the presence of metals in the underdense regions of the IGM is a distinguishing test between proposed pollution mechanisms.

The data

The ESO Large Programme (LP) "Cosmological Evolution of the IGM" (PI J. Bergeron) has been devised to gather a homogeneous sample of echelle spectra of 21 QSOs, of which 19 are at $z_Q < 4.0$, with a uniform spectral coverage, resolution and signal-to-noise ratio suitable for studying the IGM in the redshift range 1.7–4.5. The data were obtained with the Ultra-violet and Visible Echelle Spectrograph (UVES) mounted on the ESO KUEYEN 8.2 m telescope at the Paranal observatory. Spectra were obtained in service mode observations spread over two years, for
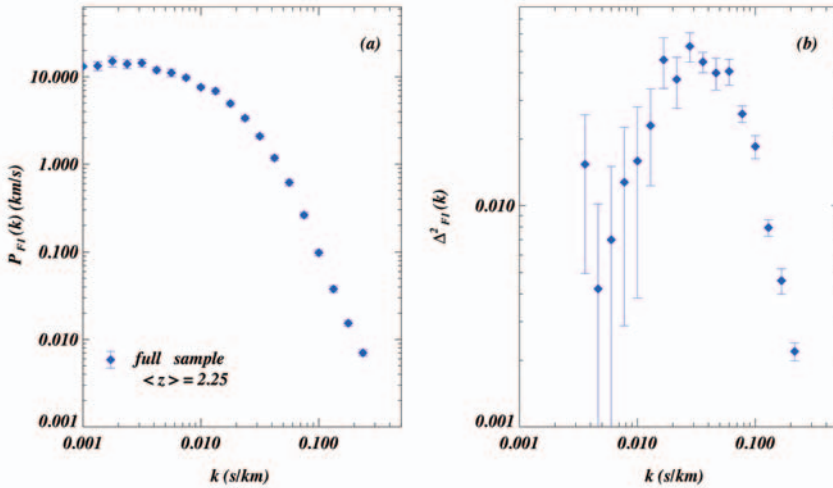
Figure 1: The 1D and 3D flux power spectrum in the Lyman-α forest.

a total of 334 h under good seeing conditions (≤ 0.8 arcsec).

The data were reduced using a version of the ESO-UVES pipeline upgraded by B. Aracil to solve problems specific to quasar spectra when the object continuum level is low (typically in the Lyman-α forest around strong absorption lines): 1) incorrect extraction of the object spectrum resulting in a lower signal-to-noise ratio than that measured on the 2D spectrum or even non-recognition of the position of the object in a given order, 2) error up to 5% on the intensity zero level, 3) non-recognition of some orders in the red, 4) strong residuals from weak sky emission lines/absorption bands in the UV after sky subtraction, 5) possibly, too large additional noise from the subtraction of the inter-order background when the object continuum is close to zero (e.g. damped Lyman lines).

With this upgraded version of the UVES data reduction pipeline, the final accuracy of the sky-background subtraction is better than 1%. Addition of individual exposures was performed using a sliding window and weighting the signal by the total errors in each pixel.

The wavelength calibration was carefully checked using the calibration lamp and it is better than $\delta\lambda/\lambda \sim 7\times10^{-7}$ rms over the full wavelength range of interest, 305–540 and 545–1000 nm. As an example of the quality of the wavelength calibration, we have found that we could obtain from the LP data better rest-wavelengths of the C IV doublet as compared to the laboratory wavelengths (Petitjean & Aracil, 2004). More details on the data redution can be found in Chand et al. (2004a) and Aracil et al. (in preparation). Signal-to-noise ratios of ~ 40 to 80 per pixel and spectral resolutions ≥ 45,000 are achieved over the wavelength range of interest.

The data analysis (identification of metal absorption lines and profile fitting) has been automated as far as possible to be able to perform the same procedures to the observed data as to simulated data constructed from *N*-body cosmological simulations.

PROBING THE MATTER DISTRIBUTION

The distribution of neutral hydrogen traces the underlying matter distribution sufficiently well that interesting constraints on the dark matter power spectrum can be obtained from the Lyman-α forest. Kim et al. (2004) have measured the power spectrum of the flux distribution in the Lyman-α forest of an augmented version of the UVES LP sample (Fig. 1).

Viel et al. (2004a) have used this flux power spectrum together with a large suite of hydrodynamical simulations to determine the dark matter power spectrum at scales of 2–20 (comoving) Mpc – a range of scales currently only probed by the Lyman-α forest. Together with constraints on large scales from CMB data important information on the power spectrum of initial density fluctu-

ations imprinted during the inflationary phase of the Early Universe can be obtained. The WMAP team has performed such an analysis and has found that the power spectrum of initial density fluctuations deviates from the canonical $n_s = 1$ power law and that a "running" of the spectral index is required. Based on the results of Kim et al. (2004), Viel et al. (2004a, 2004b) have refuted this claim and have shown that the joint analysis of the Lyman-α forest and CMB data gives results which are consistent with a Harrison-Zeldovich ($n_s = 1$) spectrum of initial density fluctuations with no evidence for a running of the spectral index as shown in Fig. 2.

METALS IN THE IGM

It is believed that the gas in the IGM traces the spatial structure of the dark matter, its overdense filaments as well as underdense voids. In the course of cosmic evolution, this gas was most likely enriched by winds flowing out from star-forming regions located preferentially in the center of massive halos. It is therefore not surprising that C IV absorption is observed to be associated with most of the strong H I lines with $N(H\ I) > 10^{14.5}$ cm^{-2}, as these lines likely trace filaments in which the massive halos are embedded. A crucial question is whether the gas filling the underdense space delineated by these filaments (the so-called voids) also contains metals. Indeed, it is improbable that winds from star-forming regions located in the filaments can pollute the voids. Therefore, if metals are found in this gas, they must have been produced by objects more or less uniformly spatially distributed, perhaps in the very early universe (z ~ 15–20).

The absorptions arising in the voids are mostly of low-column densities (typically of the order or less than $N(H\ I) = 10^{13}$ cm^{-2}). Given the low typical metallicities ([C/H] < –2.5, or 1/300 solar), direct detection of metals at such low neutral hydrogen optical depths is impossible and statistical methods must be used instead. Lu et al. (1998) used the stacking method to increase the signal-to-noise ratio and did not find any evidence
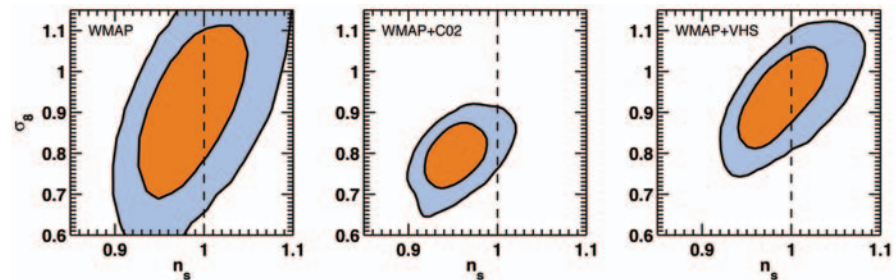

Figure 2: 1- and 2-σ likelihoods for the *rms* matter density fluctuation amplitude σ_8 and the spectral index of primordial density fluctuations n_s. The left panel shows the constraints from WMAP only. The middle panel is for a combined analysis of WMAP data and high resolution Lyman-α forest data with an effective optical depth as assumed by the WMAP team. The right panel is for a combined analysis of WMAP data and high resolution Lyman-α forest data with a Lyman-α effective optical depth suggested by high S/N, high-resolution data.

Figure 3: C IV (top panel) and O VI (bottom panel) optical depth versus H I optical depth for $z < 2.4$ (filled circles and solid line) and $z > 2.4$ (triangles and dashed line).
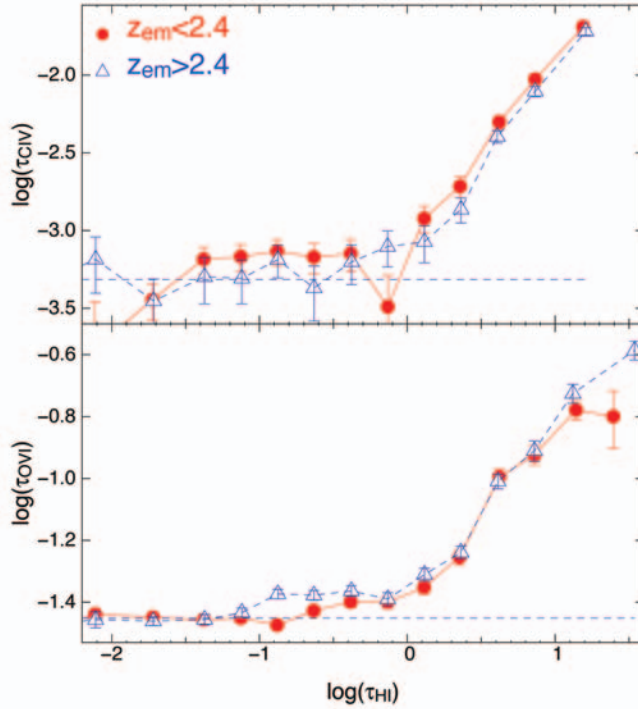
for metals in the range $10^{13} < N(\text{H I}) < 10^{14}$ cm^{-2}. Although uncertainties in the position of the lines can lead to underestimate the absorption, they concluded that metallicity is smaller than 10^{-3} solar in this gas. Cowie & Songaila (1998) calculated the C IV optical depth corresponding to each pixel of the Lyman-α forest (see Aguirre et al. 2002 for an extensive discussion of the method). They showed that the mean C IV optical depth correlates with τ_{HI} for $\tau_{\text{HI}} > 1$.

We have applied a slightly modified version of the method introduced by Cowie & Songaila (1998) to the very high quality data of the LP (Aracil et al., 2004). We find that the gas is enriched in carbon and oxygen for neutral hydrogen optical depths $\tau_{\text{HI}} > 1$ but, contrary to previous claims, there is no indication that C IV absorption is statistically associated with gas of $\tau_{\text{HI}} < 1$ (see Fig. 3). In addition, our observations strongly suggest that the C IV/H I ratio decreases with decreasing τ_{HI} with log $\tau_{\text{CIV}} = 1.3$ log $\tau_{\text{HI}} - 3.2$, which leads to log (C IV/H I) < -3.3 for $\tau_{\text{HI}} < 1$. However, we observe that a small fraction of the low density gas is associated with strong metal lines as a probable consequence of the IGM enrichment being highly inhomogeneous.

We detect the presence of O VI down to $\tau_{\text{HI}} \sim 0.2$, and the correlation between τ_{OVI} and τ_{HI} is consistent with a constant ratio log(O VI/H I) ~ -2.0 (Aracil et al., 2004). We show that O VI absorption in the lowest density gas, $0.2 < \tau_{\text{HI}} < 1$, is located within ~ 300 km/s from strong H I lines (see Fig. 4). This suggests that this O VI phase may be part of winds flowing away from overdense regions. There is no O VI absorption, at $\tau_{\text{HI}} < 1$, associated with gas located at velocities larger than ~ 300 km/s away from strong absorption lines. Therefore, at the limit of present surveys, the presence of metals in the underdense regions of the IGM, is still to be demonstrated.

CLUSTERING OF INTERGALACTIC METALS

A second approach constraining the enrichment history of the IGM is to study the spatial clustering of metals. The main sample used comprises 643 C IV components with $N \geq 10^{12}$ cm^{-2} detected over 19 ($z_Q < 4.0$) LP sightlines. This sample was first used to derive the C IV column density distribution function $f(N)$ for two redshift bins, 1.5–2.3 and 2.3–3.1 (Pichon et al., 2003). This distribution does not evolve with redshift, as found by previous studies and is consistent with a power-law of the form $f(N) \propto N^{-1.8}$.

We then computed the C IV line-of-sight two-point correlation function in redshift space, using a sample based on 580 components with $N \geq 10^{12}$ cm^{-2} (Scannapieco et al., in preparation). This number differs slightly
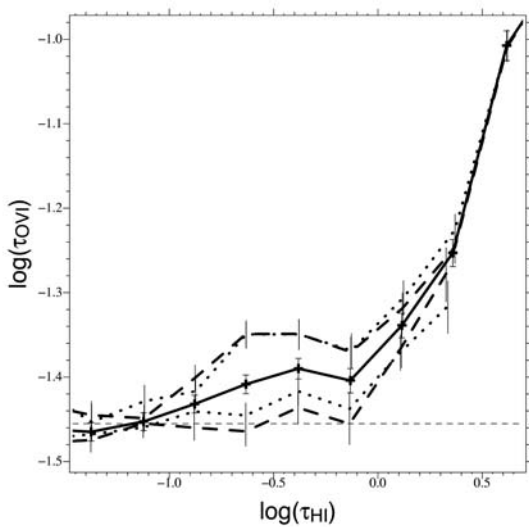

Figure 4: Median O VI optical depth versus median H I optical depth for pixels located at less than 500 km/s (upper dashed curve) or less than 300 km/s (upper dotted curve) from strong absorptions ($\tau_{\text{HI}} > 4$) and for pixels located at more than 500 km/s (lower dashed curve) or more than 300 km/s (lower dotted curve) from strong absorptions.
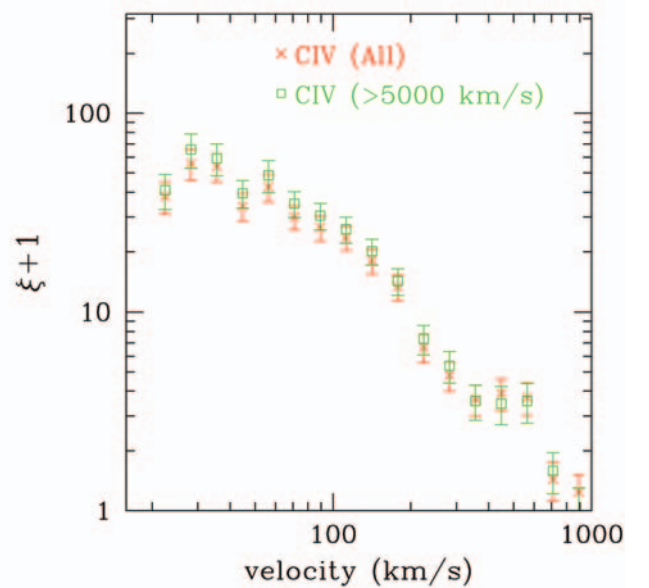

Figure 5: C IV correlation function for the whole sample (crosses) and excluding systems with velocity differences smaller than 5000 km/s compared to the QSO emission redshift (squares).
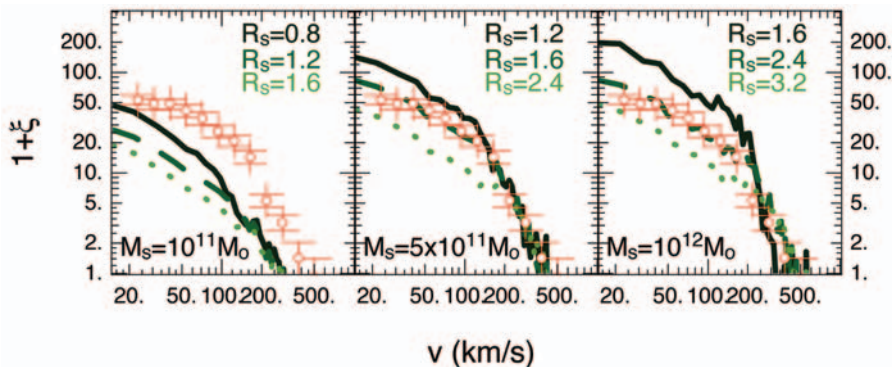
Figure 6: Comparison between detected C IV correlation functions (points) and simulated correlations (lines). In each panel the total mass M_s is fixed and the radius R_s (Mpc) is varied over three representative values.

from that mentioned above due to further refinements in the detection procedure. It should be noted that, as pixel methods are not suited to studying clustering, this analysis can only be carried out on the $\tau_{CIV} \geq 0.05$ components that can be well detected by Voit-profile fitting. The results are shown in Fig. 5: the features present in this correlation function are independent of optical depth and illustrate three important aspects of enrichment uncovered by our measurements.

At small velocity separations, $v \leq 100$ km/s, the correlation function is relatively flat, suggesting that metals are contained primarily within ~1 comoving Mpc h^{-1} from the sources, and within potential wells with velocity dispersions ~100 km/s.

At larger velocity separations, the C IV correlation function is steep and similar in shape and amplitude to that of the brightest Lyman-break galaxies. This is a clear indication of enrichment from overdense sources: either massive galaxies at late times, or dwarf galaxies at high redshifts. Finally, at the largest separations $(400 < v < 600$ km/s) there is a plateau in the correlation function possibly caused by the internal velocity dispersion between C IV systems in forming groups and clusters at z ~ 2.5.

The two-slope shape of the C IV correlation function is suggestive of a picture in which metal bubbles of a typical size (associated with the small scale clustering) are generated about objects of a typical mass (whose geometrical bias is associated with the large-scale clustering). In order to explore this connection further, we generated a simple model, based on a dark-matter-only simulation (Pichon et al., 2003).

We found that the measured correlation function is consistent with a picture where, at $z = 3$, metals are confined within bubbles of R_s ~ 2 Mpc about halos of total mass M_s ~5 10^{11} M$_\odot$ (see Fig. 6). This implies that the filling factor of the metals is only ~10% at the detection limit of the survey.

INTERGALACTIC O VI

The recent searches for O VI individual absorbers aim at probing low-density regions of the IGM with gas overdensities of $\rho/\bar{\rho} < 10$, where $\bar{\rho}$ is the cosmic mean density. These tenuous regions of the IGM are photoionized by the metagalactic UV flux and their ionization level should be higher than those of the regions usually traced solely by C IV. The goals are to derive the ionization level, metallicity and gas density of the IGM O VI phase, constrain the spectral shape of the UV ionizing flux, and estimate the contribution of the high ionization phase to the baryon cosmic density Ω_b.

The O VI $\lambda\lambda$1031.9,1037.6 doublet is more difficult to detect than that of C IV due to severe contamination by the Lyman forest lines. This leads to a reduction of the usable redshift path by at least a factor of two already at $z \sim 2.3$. Unambiguous detections can be made for column densities $N(O\ VI) \geq 1.5\ 10^{13}$ cm^{-2}, or $\tau_{OVI} \geq 0.3$ for a Doppler parameter $b = 10$ km/s.

The heating source of the O VI absorbers can be constrained by their O VI line widths. For Doppler parameters $b(O\ VI) < 10$ [14] km/s, the derived temperatures are $T < 1$ [2] 10^5 K. In the assumption of shock heating, this leads to very small O VI ionic ratios, O VI/O $< 6\ 10^{-8}$ [2 10^{-2}] (Sutherland & Dopita, 1993), and consequently super-solar metallicities (Bergeron et al., 2002). Among the absorbers of

low N(H I) $(< 10^{15}$ cm$^{-2})$, there are many clear cases of O VI lines with $b < 10$ km/s, thus photoionized gas (Bergeron et al., 2002; Carswell et al., 2002). An example with $b(O\ VI) = 9.5$ km/s is shown in Fig. 7. The distribution of the O VI Doppler parameter is presented in Fig. 8 for the currently analyzed O VI sub-sample. About half of the systems have $b < 14$ km/s which implies that radiative ionization is then the dominant process. Among the remaining systems, most are weak, thus possibly blends of narrower lines, but there are also systems with large N(H I). For the latter, the possibility of shock heating was suggested by Simcoe et al. (2002) and this remains an open issue.

For a given ionizing background flux, the O VI/N V/C IV ionic ratios (including limits) can be used to estimate the ionization parameter, thus the gas density and path-length of the absorbers, and the metal abundances, thus constraining the [O/C] abundance ratio. We find that the observed ionic ratios are best reproduced by a hard ionizing
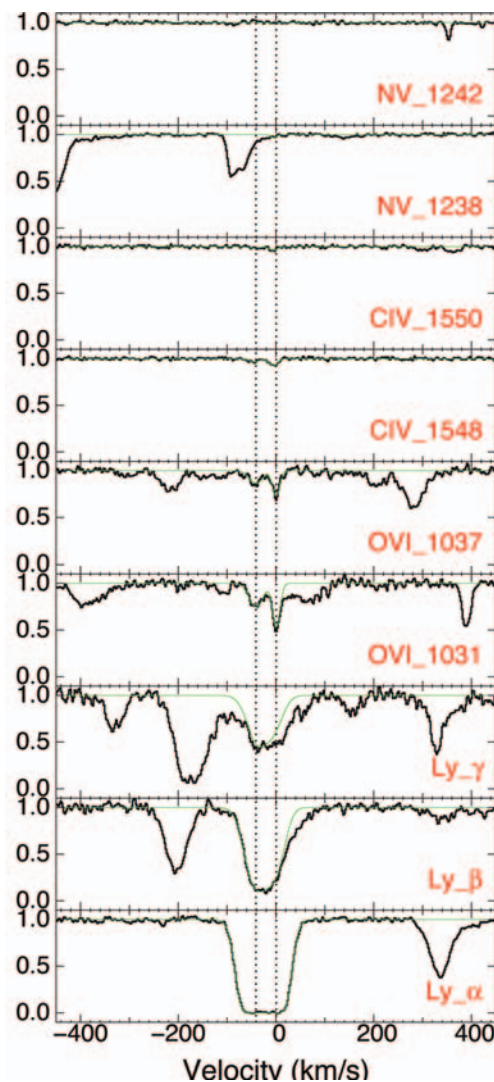

Figure 7: Normalized flux versus velocity of Lyman and metal lines for the system at $z = 2.36385$ in Q 0329–385 (thick lines) together with the best fit model (thin lines).
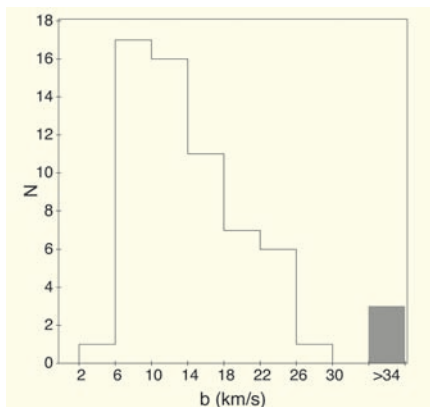
Figure 8: Histogram of the O VI doublet *b* values.

spectrum and the derived [O/C] abundance ratio depends on the spectral energy distribution of the UV flux. Even for a hard spectrum (break at 4 Ryd of about 3), a supersolar [O/C] relative abundance is needed in some cases which suggests that massive stars are a dominant source of metal enrichment of the IGM. The range in metallicity is large, $\sim 10^{-3}$ to 10^{-1} solar, which implies very inhomogeneous metal enrichment.

The observed ionic ratios can also be analyzed using a relation between H I column density and gas density, n_H, which assumes hydrostatic equilibrium and photoionization. In this alternative approach, the observed ionic ratios constrain the spectral dependence of the ionizing flux for a given [O/C] abundance ratio. For absorbers with $N(H\ I) \geq 10^{13.5}$–10^{-15} cm^{-2}, the values derived for the gas density by the two methods are within a factor of 2–3, but for smaller $N(H\ I)$ this is not the case: the values derived from photoionization models are much larger than those using the n_H–$N(H\ I)$ relation. The latter include cases with or without detection of N V and may comprise absorbers of a different nature.

We are currently analyzing a O VI sample with $N(O\ VI) \gg N(C\ IV)$, no associated N V and covering a wide range of $N(H\ I)$ (an example is the $z = 2.24835$ system in Q 0329–385 presented by Bergeron et al., 2002). These absorbers have a high ionization level and we will investigate whether any probe the more tenuous regions of the IGM.

ABUNDANCE PATTERNS IN SUB-DLAs

Next to the diffuse, photoionised IGM that gives rise to the Lyman-α forest, H I-rich absorbers represent important objects to study the metal enrichment history of the Universe. At $z > 1$, the Damped Lyman-α systems (DLAs), N(H I) $\geq 2\ 10^{20}$ cm^{-2}, con-

tain most of the neutral gas mass in the Universe and it is believed that they represent the progenitors of present-day galaxies. The excellent signal-to-noise ratio and high spectral resolution of the LP sample allows us to study sub-DLAs, $10^{19} < N(H\ I) < 2\ 10^{20}$ cm^{-2}, in great detail, a population not yet fully investigated. We have recently analysed two sub-DLAs at $z = 2.2$ and $z = 3.1$ toward HE 0001-2340 and Q 0420+388, respectively (Richter et al., 2004). A large number of ions are detected, including O I and N I. Both systems show a large number (>12) of velocity subcomponents spread over several hundred km/s, implying a complex structure of the absorbing gas.

Most interesting are the derived abundance trends for the CNO elements. For the sub-DLA toward HE 0001-2340, we find [O/H]=–1.81± 0.07, [N/H]≤ –3.3, and [N/O] ≤ –1.5 and this absorber is among the systems with the lowest ever measured [N/α] ratios. This result is consistent with the idea that primary nitrogen production by the very first stars have enriched the intergalactic gas to a level of [N/O] $\approx$ –1.5. Peculiar overabundances of a number of species such as Si, Al, and P are found in the outermost blue velocity components. Possibly, the line of sight toward HE 0001-2340 may pass through the gaseous environment of stellar clusters that locally enriched their interstellar neighbourhood by supernova ejecta.

The preliminary analyis of the z=3.1 sub-DLA toward Q 0420+388 shows that this system consists of two individual groups of absorbers, separated by ~100 km/s, that appear to have different oxygen abundances ([O/H] $\approx$–0.7 and –1.2). The relatively high overall abundance has led to the detection of a number of interesting ions such as Si I, Ni II, and Zn II. A detailed analysis of this sub-DLA is in progress.

The abundance variations and large velocity spread of individual subcomponents in these two sub-DLAs suggest that either recent star formation activity and/or merging of several individual galaxies/protogalactic structures with different chemical enrichment histories has led to an inhomogeneous distribution of heavy elements in the gas.

CONSTRAINING THE VARIATIONS OF THE FINE-STRUCTURE CONSTANT

Constraints on the possible time variation of the fine-structure constant, α, have been recently reported in a previous issue of the *Messenger* (Srianand et al., 2004a). This has important implications for some new theories of fundamental physics which require the existence of extra spatial dimensions and allow for a cosmic evolution of their scale size.

As the energy of the atomic transitions depend on α, the time evolution of α can be probed by measuring possible small shifts in the absorption line spectra seen toward high redshift QSOs and comparing them to its value on Earth.

This method, applied to a large heterogeneous sample of QSO absorption lines, has resulted in the claim for a smaller value of α in the past, $\Delta\alpha/\alpha$ =(–0.574± 0.102) 10^{-5} for $0.2 \leq z \leq 3.7$ (Murphy et al., 2003 and references therein). Using the LP data, Srianand et al. (2004b) and Chand et al. (2004a) have however derived the more stringent constraint $\Delta\alpha/\alpha$ = (–0.06±0.06) 10^{-5} over the redshift range $0.4 \leq z \leq 2.3$. The corresponding 3σ upper limit on the time variation of α is –2.5 10^{-16} yr^{-1} $\leq$ ($\Delta\alpha/\alpha\Delta t$) $\leq$ +1.2 10^{-16} yr^{-1}, in the most favored cosmological model today. This does not support the previous claims of a statistically significant change in $\Delta\alpha/\alpha$ with cosmic time at $z > 0.5$.

Recently, we conducted a similar analysis on a sample of 15 Si IV doublets selected from the LP data, extending the probed redshift range up to $z \sim 3$. We obtained a value $\Delta\alpha/\alpha$= (+0.15±0.43) 10^{-5} over the redshift range $1.59 \leq z \leq 2.92$ which, as at lower redshift, is consistent with no variation of α (Chand et al., 2004b).

REFERENCES

Aguirre, A., Schaye, J., & Theuns, T., 2002, ApJ, 576, 1

Aracil, B., Petitjean, P., Pichon, C., & Bergeron, J., 2004, A&A, 419, 811

Bergeron, J., Aracil, B., Petitjean, P., & Pichon, C., 2002, A&A, 396, L11

Carswell, B., Schaye, J., & Kim, T.-S., 2002, ApJ, 587, 43

Chand, H., Srianand, R., Petitjean, P., & Aracil, B., 2004a, A&A, 417, 853

Chand, H., Petitjean, P., Srianand, R., & Aracil, B., 2004b, A&A, in press, astro-ph/0408200

Cowie, L. L., & Songaila, A., 1998, Nature, 394, 44

Kim, T.-S., Viel, M., Haehnelt, M. G., Carswell, R. F., & Cristiani, S., 2004, MNRAS, 347, 355

Lu, L., Sargent, W. L. W., Barlow, T. A., & Rauch, M., 1998, astro-ph/9802189

Murphy, M. T., Webb, J. K., & Flambaum, V. V., 2003, MNRAS, 345, 609

Petitjean, P., & Aracil, B., 2004, A&A, 422, 523

Pichon, C., Scannapieco, E., Aracil, B., Petitjean, P., Aubert, D., Bergeron, J., & Colombi, S., 2003, ApJ 597, L97

Richter, P., Ledoux, C., Petitjean, P., & Bergeron, J., 2004, A&A, submitted

Simcoe, R. A., Sargent, W. L. W., & Rauch, M., 2002, ApJ, 578, 737

Srianand, R., Petitjean, P., Chand, H., & Aracil, B., 2004a, Messenger, 116 , 25

Srianand, R., Chand, H., Petitjean, P., & Aracil, B., 2004b, PhRvL, 92, 12130

Sutherland, R. S., & Dopita, M. A., 1993, ApJS, 88, 253

Viel, M., Haehnelt, M. G., & Springel, V., 2004a, MNRAS, 354, 684

Viel, M., Weller, J., & Haehnelt, M. G., 2004b, MNRAS, in press, astro-ph/0407294